

# Towards Adversarial Training under Hyperspectral Images

Weihua Zhang<sup>1</sup>, Chengze Jiang<sup>1</sup>, Jie Gui<sup>1</sup>, Lu Dong<sup>1</sup>

<sup>1</sup>Southeast University

zwhseu@seu.edu.cn, czjiang@seu.edu.cn, guijie@ustc.edu, ldong90@seu.edu.cn

## Abstract

Recent studies have revealed that hyperspectral classification models based on deep learning are highly vulnerable to adversarial attacks, which pose significant security risks. Although several approaches have attempted to enhance adversarial robustness by modifying network architectures, these methods often rely on customized designs that limit scalability and fail to defend effectively against strong attacks. To address these challenges, we introduce adversarial training to the hyperspectral domain, which is widely regarded as one of the most effective defenses against adversarial attacks. Through extensive empirical analyses, we demonstrate that while adversarial training does enhance robustness across various models and datasets, hyperspectral data introduces unique challenges not seen in RGB images. Specifically, we find that adversarial noise and the non-smooth nature of adversarial examples can distort or eliminate important spectral semantic information. To mitigate this issue, we employ data augmentation techniques and propose a novel hyperspectral adversarial training method, termed AT-RA. By increasing the diversity of spectral information and ensuring spatial smoothness, AT-RA preserves and corrects spectral semantics in hyperspectral images. Experimental results show that AT-RA improves adversarial robustness by 21.34% against AutoAttack and 18.78% against PGD-50 while boosting benign accuracy by 2.68%.

## 1 Introduction

Driven by the development of deep learning models, significant progress has been made in the field of hyperspectral image scene classification [Chen *et al.*, 2016; Mou *et al.*, 2017; Zhang *et al.*, 2021; Roy *et al.*, 2023]. Although deep learning models have achieved great success in the remote sensing community, their adversarial robustness seems to be neglected [Zhang *et al.*, 2022; Xiao *et al.*, 2022; Han *et al.*, 2023; Yang *et al.*, 2024]. Recently, a few researchers have shown that with the unique spectral characteristics of hyperspectral data, deep learning models on the hyperspectral im-

age classification task are also subjected to the potential threat of adversarial examples [Xu *et al.*, 2021b; Bai *et al.*, 2022; Xu *et al.*, 2023a; Shi *et al.*, 2023; Shi, 2024]. Therefore, employing adversarial defense methods is a critical security measure.

Currently, most researchers in the remote sensing field focus on designing robust deep neural networks to enhance the resistance to adversarial examples [Gu and Rigazio, 2015; Ross and Doshi-Velez, 2018; Tu *et al.*, 2023; Qi *et al.*, 2024; Xu *et al.*, 2024]. However, these approaches alter the original structure of the deep learning models, limit the input data, and fail to explore the spectral nature of adversarial examples, leading to limited scalability without significantly improving adversarial robustness. To address these challenges, adversarial training (AT), as an alternative defense method, has gradually gained attention in the research community. It is widely regarded as one of the most effective approaches to defend against adversarial attacks [Bai *et al.*, 2021]. In the remote sensing domain, the traditional adversarial training strategy [Xu *et al.*, 2021a] has yielded promising results in the fields of SAR and optics. However, there is only a few relevant research in the hyperspectral domain, and whether adversarial training can be effectively applied to hyperspectral data remains an open question.

Therefore, we are committed to exploring the effect of adversarial training in the hyperspectral domain and further developing tailored strategies to enhance its performance. We choose the traditional remote sensing adversarial training strategy [Xu *et al.*, 2021a] and its components as the baseline to evaluate the robustness of hyperspectral classification models. The results demonstrate that adversarial training shows its effectiveness in resisting powerful adversarial attacks such as PGD-50 [Madry *et al.*, 2019] and AA [Croce and Hein, 2020]. However, the hyperspectral data introduces unique spectral characteristics not seen in RGB images, which also extend to the adversarial training. We conduct spectral analysis on both benign and adversarial examples, revealing that adversarial noise and the non-smooth nature of adversarial examples distort or eliminate critical spectral semantic information, which we refer to as the classification imbalance issue. To address this issue, we employ data augmentation techniques. By incorporating RandAugment, we propose a novel adversarial training method called **AT-RA**. This approach enhances the diversity of spectral-domain informa-

tion and ensures spatial smoothness, thereby preserving and restoring critical spectral semantic information in hyperspectral images. Consequently, AT-RA effectively mitigates the classification imbalance issue.

Through extensive experiments, we demonstrate that AT-RA significantly improves adversarial robustness, achieving a 21.34% increase against AutoAttack and an 18.78% increase against PGD-50, while also boosting benign accuracy by 2.68%. Furthermore, these improvements apply to both traditional adversarial training methods and fast adversarial training (FAT) methods.

Our contributions can be summarized as follows.

- We introduce adversarial training into the hyperspectral domain. We validate its effectiveness, achieving substantial improvements in adversarial robustness over traditional remote sensing adversarial training strategy.
- We perform an in-depth spectral analysis, identifying the classification imbalance issue caused by adversarial perturbations. To address this, we incorporate RandAugment and propose a novel hyperspectral adversarial training method, AT-RA.
- We conduct extensive ablation studies and validate the necessity of combining multiple data augmentation strategies.

## 2 Related Work

### 2.1 Adversarial Defense in the Hyperspectral Domain

Adversarial attacks involve introducing subtle, human-imperceptible perturbations to input examples, with the aim of misleading deep learning models into producing incorrect predictions [Jiang *et al.*, 2020; Shi *et al.*, 2022; Xu *et al.*, 2023b; Bai *et al.*, 2024]. These perturbed inputs are commonly referred to as adversarial examples. The emergence of adversarial examples has highlighted significant security vulnerabilities in deep learning models [Zhang and Zhang, 2022; Lu *et al.*, 2022; Zhang *et al.*, 2023; Zhu *et al.*, 2024]. As a result, the remote sensing community has devoted increasing attention to developing effective defense mechanisms against adversarial attacks [Yang *et al.*, 2021; Qi *et al.*, 2023; Yu *et al.*, 2024].

In the hyperspectral domain, most research on adversarial defenses has concentrated on designing robust network architectures to capture global spatial relationships and improve intrinsic model robustness. For instance, [Tu *et al.*, 2023] introduced the Robust Class Context-Aware Network, which employs a supervised affinity loss to distinguish intra-class and inter-class contextual information. Similarly, [Qi *et al.*, 2024] proposed a framework combining random input masks with graph-based self-supervised learning to construct a robust architecture. Additionally, [Xu *et al.*, 2024] developed the Spatial-Spectral Self-Attention Network ( $S^3$ ANet), which leverages pyramid-based spatial and global spectral relationships to enhance adversarial robustness in hyperspectral image classification.

Despite these advancements, the limitations of such approaches are evident. These methods often modify the orig-

inal deep learning model architecture, restrict input data formats, and fail to fully explore the spectral properties of adversarial examples. Consequently, their scalability is limited, and their effectiveness in improving adversarial robustness remains suboptimal.

### 2.2 Adversarial Training

Adversarial training, initially proposed by [Goodfellow *et al.*, 2014], is a well-established method for defending against adversarial examples. It is widely regarded as one of the most principled defense strategies against adversarial attacks [Akhtar *et al.*, 2021]. In this approach, models are trained using both benign and adversarial examples, enabling them to learn to counteract various forms of adversarial attacks and thereby improving robustness and generalization in real-world scenarios. [Madry *et al.*, 2019] formalized adversarial training as a min-max optimization problem, expressed mathematically as

$$\min_{\theta} \mathbb{E}_{(x,y) \sim D} \left[ \max_{\delta \in [-\xi, \xi]} \mathcal{L} \left( f \left( x' ; \theta \right) , y \right) \right], \quad (1)$$

where  $x' = x + \delta$ ,  $\delta$  represents adversarial perturbation generated by various attack methods;  $D$  denotes the data generator. From Equation 1, it is evident that the choice of attack method for generating adversarial examples plays a critical role in determining the reliability of adversarial training.

Adversarial training methods are generally categorized into two types: FGSM-based adversarial training and PGD-based adversarial training. FGSM-based training, also known as fast adversarial training, emphasizes computational efficiency while retaining robust performance.

In the remote sensing field, the adversarial training strategy [Xu *et al.*, 2021a] has shown promising results in SAR and optical remote sensing images. However, there has been no related research in the hyperspectral domain, and whether adversarial training can be effectively applied to hyperspectral images remains an open question. Given the inherent efficiency and generalizability of adversarial training, investigating its applicability to hyperspectral images is both a valuable and practical endeavor.

## 3 Adversarial Training for Hyperspectral Images

### 3.1 Preliminaries

Compared to the adversarial training method [Madry *et al.*, 2019], the traditional remote sensing adversarial training strategy [Xu *et al.*, 2021a] incorporates two additional components: 1) a benign example pretraining module (BEPM), and 2) an adversarial-benign loss module (ABL).

**Benign Example Pre-training Module** The primary concept of the traditional remote sensing adversarial training strategy is to train deep neural networks on a combination of benign and adversarial examples [Xu *et al.*, 2021a]. This process begins with the inclusion of a BEPM before the adversarial training stage, allowing the model to learn more feature

Method	Components		Accuracy						Time (s)
	BEPM	ABL	Benign	FGSM	PGD-10	PGD-50	CW	AA	
AT			97.09	<b>91.66</b>	<b>84.36</b>	<b>75.33</b>	<b>90.53</b>	<b>72.85</b>	<b>231</b>
AT-BEPM	✓		88.00	49.64	37.88	37.03	45.99	30.59	374
AT-ABL		✓	<b>97.23</b>	75.82	65.39	63.21	74.70	61.01	271
AT-ABL-BEPM	✓	✓	86.82	40.61	30.42	28.83	39.98	25.22	380

Table 1: Benign accuracy, adversarial robustness, and training time of different components on Pavia University dataset using ResNet-18 [He *et al.*, 2016] when traditional remote sensing adversarial training strategy is used for adversarial training, where the best results have been bolded.

representations from benign examples. The process is mathematically expressed as

$$\begin{aligned} & \arg \min_{\theta_{pt}} \mathcal{L}_{\text{adv}}(\theta_{pt}; x', y), \\ & \text{where } \theta_{pt} = \arg \min_{\theta} \mathcal{L}_{\text{ben}}(\theta; x, y), \\ & x' = \arg \max_{\|x' - x\|_p \leq \epsilon} \mathcal{L}_{\text{ben}}(\theta_{pt}; x', y), \end{aligned} \quad (2)$$

Where,  $\theta$  represents the initial parameters of the model, and  $\theta_{pt}$  denotes the parameters of the model after pre-training with benign examples.  $x'$  represents the adversarial example generated from the benign example  $x$  under the  $L_p$ -norm constraint, with  $y$  being the label of  $x$ .  $\mathcal{L}_{\text{ben}}$  denotes the classification loss function of the model, and  $\mathcal{L}_{\text{adv}}$  represents the adversarial loss function.

**Adversarial-Benign Loss Module** To ensure that both the benign example  $x$  and its corresponding adversarial example  $x'$  are assigned the same true label  $y$ , the traditional remote sensing adversarial training strategy combines adversarial and benign losses with equal weights, which is the Adversarial-Benign Loss (ABL). The mathematical expression for the ABL is

$$\mathcal{L}_{\text{adv}}(\theta; x, y) = \mathcal{L}_{\text{ben}}(\theta; x', y) + \mathcal{L}_{\text{ben}}(\theta; x, y). \quad (3)$$

In the specific implementation, the traditional remote sensing adversarial training strategy chooses the cross-entropy function as the classification loss function  $\mathcal{L}_{\text{ben}}$  for the model. The mathematical expression is

$$\mathcal{L}_{\text{ben}}(\theta; x, y) = y \log(f(x)) + (1 - y) \log(1 - f(x)). \quad (4)$$

### 3.2 Effects of Different Components

We transfer the traditional remote sensing adversarial training strategy to hyperspectral images and conduct a series of experiments to investigate the effect of each component. Specifically, each component is sequentially added to the adversarial training framework to analyze its influence on benign accuracy, adversarial robustness, and training time. The results are summarized in Table 1. More details on the adversarial training process are provided in Chapter 5.

We observe that the adversarial training method outperforms the traditional remote sensing adversarial training strategy [Xu *et al.*, 2021a] in terms of adversarial robustness and training time. Although AT-ABL can improve benign accuracy, it significantly reduces the adversarial robustness when facing adaptive attacks such as CW [Carlini and Wagner,

2017] and AA [Croce and Hein, 2020], while also increasing the training time.

Meanwhile, we also conduct the same experiments on the fast adversarial training method [Wong *et al.*, 2020], and the results are detailed in the Appendix. We observe that even when using fast adversarial training, the experimental results were consistent with those obtained from the adversarial training method.

These observations align with the conclusions of [Lin *et al.*, 2024], which indicate that continuous learning in high-confidence modes fails to enhance the model's generalization ability but even reduces it. The reason behind this phenomenon is that both the BEPM and the ABL increase the model's confidence in benign example sets, thereby diminishing its generalization ability on adversarial examples and consequently reducing adversarial robustness. The two components proposed by the traditional remote sensing adversarial training strategy do not significantly improve the benign accuracy and adversarial robustness but add to the training time. Therefore, we recommend adopting adversarial training in the hyperspectral domain, which is more efficient without sacrificing significant performance.

### 3.3 Limitation of Adversarial Training

Despite the advantages of adversarial training over traditional remote sensing adversarial training strategies in the hyperspectral domain, several limitations are identified during our experiments. The most significant of these is the classification imbalance issue.

Table 2 illustrates the classification performance of adversarial training on the Pavia University dataset.

Class ID	Class Name	Benign	Adversarial
1	Asphalt	99.92	90.03
2	Meadows	99.70	<b>81.17</b>
3	Gravel	100.0	91.94
4	Trees	99.78	93.23
5	Metal sheets	100.0	100.0
6	Bare soil	<b>76.80</b>	<b>65.57</b>
7	Bitumen	100.0	99.03
8	Bricks	99.91	93.91
9	Shadows	100.0	98.76

Table 2: Classification performance of adversarial training in Pavia University dataset.

The results indicate that the 'Meadows' class exhibits sig-

nificantly lower adversarial robustness than other classes, while both benign and adversarial accuracies for the ‘Bare soil’ class are relatively low. This phenomenon is referred to as classification imbalance issue. The classification imbalance issue observed in hyperspectral adversarial training negatively impacts both the benign accuracy and the adversarial robustness of the model.

Therefore, investigating the causes of the classification imbalance issue in adversarial training on hyperspectral images and mitigating its negative impact on both benign accuracy and adversarial robustness is a critical problem that needs to be addressed.

## 4 Study of the Classification Imbalance Issue

Due to the relatively low benign accuracy and adversarial robustness of the ‘Bare soil’ class, the classification imbalance issue has the most severe impact on this class. Therefore, we first investigate the model’s performance in classifying examples labeled as ‘Bare soil’. The classification results for benign and adversarial examples labeled as ‘Bare soil’ are shown in Table 3.

Class ID	Class Name	Benign	Adversarial
1	Asphalt	0	271
2	Meadows	<b>1097</b>	<b>1517</b>
3	Gravel	0	0
4	Trees	0	102
5	Metal sheets	0	1
6	Bare soil	3632	2800
7	Bitumen	0	19
8	Bricks	0	19
9	Shadows	0	0

Table 3: Classification of the class labeled ‘Bare soil’ in the Pavia University dataset after adversarial training. The data in the table represent the class labeled ‘Bare soil’ but is classified as the number of corresponding horizontal axis categories.

As shown in Table 3, examples labeled as ‘Bare soil’ are frequently misclassified as ‘Meadows’, significantly affecting both benign accuracy and adversarial robustness. Given that hyperspectral images contain rich spectral information, we consider conducting a spectral analysis to identify the differences in spectral properties between different classes.

### 4.1 Spectral Analysis of Benign Examples

Firstly, we investigate the ‘Meadows’ class. As shown in Figure 1 (a), the spectral curve of the ‘Meadows’ class exhibits relatively low values in the first 70 bands, with a sharp increase in the last 30 bands. The reason behind this is that the Pavia University dataset contains 103 available spectral bands, covering the range from 430 nm to 860 nm. As a type of grassland vegetation, the spectral curve of the ‘Meadows’ class typically shows a distinct peak in the visible light range, known as the ‘green peak’. This phenomenon occurs because chlorophyll has a higher reflectance within the 510–690 nm range. Meanwhile, in the near-infrared bands (760–1150 nm), the spectral reflectance of grassland vegetation is

typically higher due to the penetration of radiation through chloroplasts, which is strongly reflected by the water content in intercellular spaces. However, since grassland vegetation primarily absorbs solar radiation in the red and blue light bands, absorption valleys appear in the red and blue ranges (approximately 430 nm–550 nm), leading to lower reflectance and consequently lower values in hyperspectral data acquisition.

Then, we analyze the ‘Bare soil’ class. As shown in Figure 1 (b), the spectral curve of the ‘Bare soil’ class is relatively consistent across all bands, with values primarily ranging from 1000 to 3000, without any abrupt increases or decreases. The reasons behind this is that, within the visible light range (approximately 400 nm to 700 nm), the reflectance of bare soil is relatively high, and its spectral curve is smooth, lacking distinct absorption valleys or reflection peaks. In contrast, the reflectance of bare soil in the near-infrared range (approximately 760 nm to 1150 nm) is lower, due to the strong absorption of near-infrared light by the water content and organic matter in the soil.

By comparing Figure 1 (a) and Figure 1 (b), it is evident that the values for the ‘Meadows’ class are significantly lower than those of the ‘Bare soil’ class in the first 70 bands. This indicates that, compared to the vegetation spectral curve, the reflectance of bare soil in the visible light range is notably higher than that of vegetation in the blue and red bands. The reason behind this is that vegetation strongly absorbs blue and red light for photosynthesis, whereas bare soil lacks such absorption mechanisms.

From the spectral curves of benign examples for the ‘Bare soil’ and ‘Meadows’ classes, the distinction between the two classes is visually apparent. Additionally, deep learning models can easily capture the different features of these two classes and perform successful classification. However, when the task is shifted to adversarial examples, the situation changes drastically. Therefore, we next analyze the spectral curves of adversarial examples for both the ‘Bare soil’ and ‘Meadows’ classes.

### 4.2 Spectral Analysis of Adversarial Examples

Firstly, we investigate the ‘Meadows’ class. As shown in Figure 1 (d), due to the noise introduced by adversarial attacks, the adversarial examples of the ‘Meadows’ class have lost much of their spectral semantic information compared to the benign examples. Although the ‘green peak’ is still present, it has been partially diminished and is accompanied by an offset. The elimination of spectral semantic information causes a bias in the model’s feature learning from hyperspectral images, which negatively impacts the model’s classification performance, leading to the occurrence of the classification imbalance issue.

Then, we investigate the ‘Bare soil’ class. As shown in Figure 1 (e), the adversarial examples of the ‘Bare soil’ class maintain relatively uniform values across the entire wavelength range, generally ranging from 1000 to 3000, without exhibiting abrupt increases or decreases. However, the spectral curves of these adversarial examples demonstrate a gradually increasing trend, a feature absent in benign examples. Moreover, the adversarial examples of the ‘Bare soil’

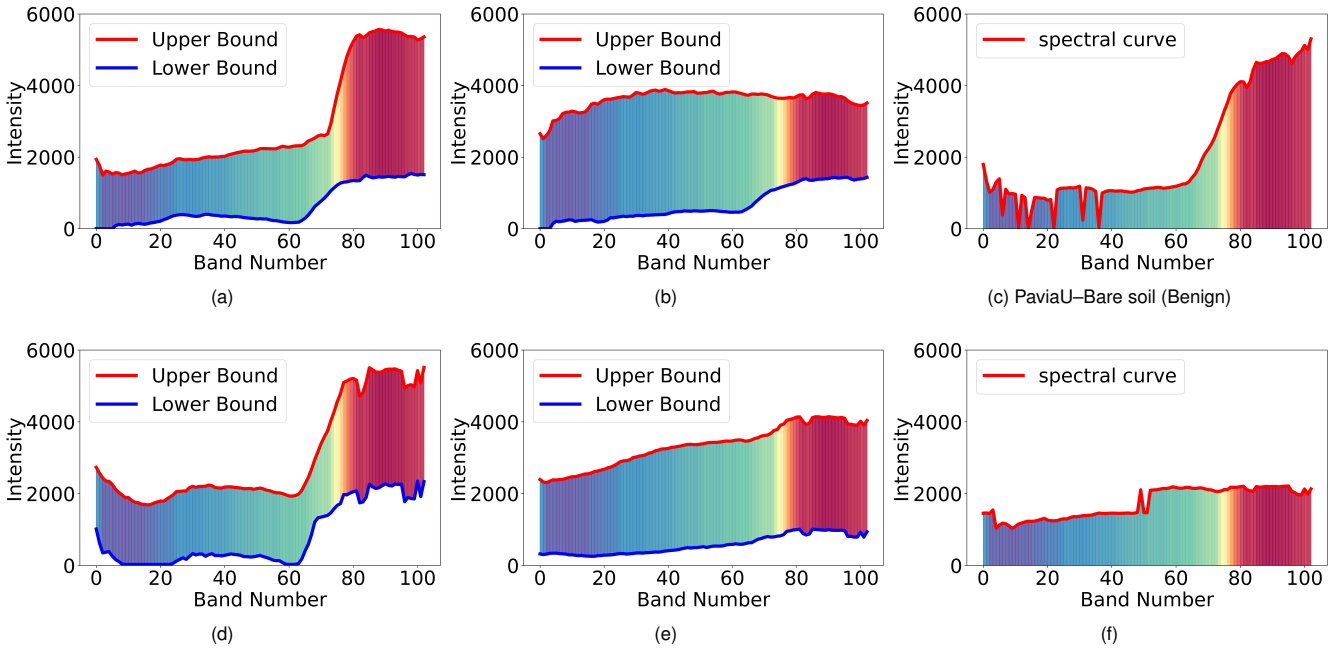


Figure 1: (a) Spectral curve of ‘Meadows’ class benign examples. (b) Spectral curve of ‘Bare soil’ class benign examples. (c) Spectral curve of an example of ‘Meadows’ adversarial examples. (d) Spectral curve of ‘Meadows’ class adversarial examples. (e) Spectral curve of ‘Bare soil’ class adversarial examples. (f) Spectral curve of an example of ‘Bare soil’ adversarial examples. ‘Upper Bound’ and ‘Lower Bound’ represent the maximum and minimum values of the intensity value on the spectrum respectively.

class show significantly lower values than the benign examples within the first 70 bands, resulting in reduced reflectance in the visible spectrum. This behavior mirrors the characteristics of the benign examples of the ‘Meadows’ class. Such distortion in spectral semantic information leads to a shift in the distribution of examples from different classes in the feature space, which subsequently results in a degradation of the model’s classification performance.

Furthermore, when combining Figure 1 (c) with 1 (f), it is evident that, compared to benign examples, the spectral curves of adversarial examples are less smooth and exhibit noticeable sawtooth patterns. The presence of adversarial noise disrupts the correlation between consecutive spectral bands in hyperspectral images. Since convolutional neural networks excel at learning local features but cannot capture global information, the unsmooth nature of adversarial examples may lead to a bias in the model’s feature learning, affecting classification performance and contributing to the occurrence of classification imbalance issue. In summary, in the spectral domain, the noise interference and unsmooth characteristics of adversarial examples lead to the elimination or distortion of spectral semantic information in hyperspectral images, which negatively impacts the model’s classification performance and, consequently, results in the occurrence of the classification imbalance issue.

### 4.3 Addressing the classification Imbalance Issue

Since the cause of the classification imbalance issue lies in the elimination or distortion of spectral semantic information in hyperspectral images due to noise interference and

the unsmooth characteristics of adversarial examples, we consider introducing data augmentation methods. This approach aims to strengthen the correlations between consecutive spectral bands, thereby preserving the distribution of examples from different classes in the feature space and mitigating the classification imbalance issue. Several studies [Carmon *et al.*, 2019; Wu *et al.*, 2020; Gowal *et al.*, 2021; Rebuffi *et al.*, 2021] have attempted to alleviate this issue through data augmentation on optical datasets, but it remains unclear whether data augmentation is still effective on hyperspectral images. Initially, we introduced state-of-the-art data augmentation techniques, including MixUp [Zhang, 2017], Cutout [DeVries, 2017], CutMix [Yun *et al.*, 2019], and AugMix [Hendrycks *et al.*, 2020], but these methods did not yield satisfactory results. Although these techniques can enhance and correct the spectral semantic information in the spectral domain, they distort the spatial semantic information in the spatial domain, resulting in unsmooth phenomena in the spatial domain and leading to the elimination of spatial relationship features in the image [Xu and Ghamisi, 2022], which in turn negatively affect the model’s performance.

Therefore, we ultimately decide to adopt the RandAugment [Cubuk *et al.*, 2020] data augmentation technique and adapt it to the hyperspectral domain to address the classification imbalance issue. RandAugment includes a total of 14 data augmentation methods, but due to the unique nature of hyperspectral images, the methods Posterize, Solarize, and Equalize cannot be transferred to the hyperspectral domain. Therefore, we select the remaining 11 methods: ShearX, ShearY, TranslateX, TranslateY, Rotate, Brightness, Color,

Method	Accuracy						Time (s)
	Benign	FGSM	PGD-10	PGD-50	CW	AA	
AT	97.09	91.66	84.36	75.33	90.53	72.85	<b>231</b>
AT-RA (ours)	<b>99.77</b>	<b>98.41</b>	<b>95.27</b>	<b>94.11</b>	<b>97.61</b>	<b>94.19</b>	1922

Table 4: Benign accuracy, adversarial robustness, and training time of RandAugment on Pavia University data set using ResNet-18 [He *et al.*, 2016] when RandAugment is applied to adversarial training. AT-RA means that the RandAugment method has been introduced into adversarial training. The best of these results have been bolded.

Contrast, Sharpness, and AutoContrast. These data augmentation techniques not only enhance the diversity of spectral domain information but also maintain smoothness in the spatial domain, allowing the model to learn richer representations.

## 5 Experiments

### 5.1 Settings

**Datasets** We conduct experiments on the Pavia University, Houston, and Washington DC datasets. Due to space constraints, only the results of the Pavia University dataset are presented in this section. The introduction, training sets configuration, as well as experimental results, are presented in the Appendix.

Class Name	Benign		Adversarial	
	AT	AT-RA	AT	AT-RA
Asphalt	99.92	100.0	90.03	99.02
Meadows	99.70	<b>99.83</b>	<b>81.17</b>	<b>93.22</b>
Gravel	100.0	100.0	91.94	99.94
Trees	99.78	98.88	93.23	96.85
Metal sheets	100.0	100.0	100.0	100.0
Bare soil	<b>76.80</b>	<b>99.47</b>	<b>65.57</b>	<b>97.44</b>
Bitumen	100.0	100.0	99.03	100.0
Bricks	99.91	99.82	93.91	98.88
Shadows	100.0	100.0	98.76	99.07

Table 5: Class-wise classification performance of RandAugment method added to adversarial training on Pavia University dataset.

**Metrics** In addition to the benign accuracy, we also evaluate the model’s adversarial robustness under an  $\epsilon = 8/255$  bounded perturbation in the  $l_\infty$  norm. The attacks used include the single-step FGSM [Goodfellow *et al.*, 2014] and multi-step iterative attacks such as PGD-10 [Madry *et al.*, 2019], PGD-50 [Madry *et al.*, 2019], and CW [Carlini and Wagner, 2017], all with a step size of 2/255. Furthermore, we also utilize AutoAttack (AA) [Croce and Hein, 2020], which is considered one of the strongest attacks.

**Details** We use the Stochastic Gradient Descent (SGD) optimizer to train the model, with an initial learning rate of 0.1, momentum of 0.9, and weight decay of 5e-4. The batch size is set to 128. The training is conducted for 50 epochs, with the learning rate reduced to one-tenth of the original value at the 40th and 45th epochs. For adversarial example generation, we set up adversarial training to generate adversarial examples with a maximum perturbation of 8/255 and a step size of

2/255, using 5 iterations for internal maximization. Additionally, we also conduct tests on fast adversarial training, where adversarial examples are generated using FGSM attacks with a maximum perturbation of 8/255 and a step size of 8/255.

### 5.2 Main Results

We re-implement RandAugment at the hyperspectral level and conduct a series of adversarial training experiments. The experimental results for adversarial training are shown in Table 4. Notably, as seen in Table 4, compared to standard AT, our method not only increases the average adversarial robustness by 12.97% but also improves benign accuracy by 2.68%. In addition, the adversarial robustness increases by 21.34% when subject to powerful attacks such as AA [Croce and Hein, 2020], and improves by 7.08% when facing adaptive attacks such as CW [Carlini and Wagner, 2017] under AT-RA. It is obvious that our method significantly enhances the model’s benign accuracy and adversarial robustness. However, this substantial improvement comes at a cost, as the training time of our method is 8.32 times longer than that of adversarial training.

Next, we investigate the effect of incorporating the RandAugment method into adversarial training on the resolution of the classification imbalance issue. The class-wise classification results on the Pavia University dataset are summarized in Table 5. Notably, as seen in Table 5, compared to standard AT, the adversarial robustness of the ‘Meadows’ class increases by 12.05% under AT-RA. Furthermore, the ‘Bare soil’ class exhibits a significant improvement, with a 31.87% increase in adversarial robustness and a 22.67% improvement in benign accuracy under AT-RA. These results demonstrate that our method effectively mitigates the negative impact of classification imbalance on both benign accuracy and adversarial robustness.

Meanwhile, we conduct the same experiments on the fast adversarial training method [Wong *et al.*, 2020], the results are summarized in Appendix. Our proposed method is also effective in fast adversarial training.

The above experiments demonstrate that our method significantly alleviates the classification imbalance issue, substantially improving the model’s benign accuracy and adversarial robustness. Moreover, it applies to both adversarial training and fast adversarial training. However, a drawback of the method is that, along with these performance improvements, the training time is also increased.

### 5.3 Ablation Study

**Investigation on the Individual Effects of Data Augmentation Methods** For each training image, RandAugment

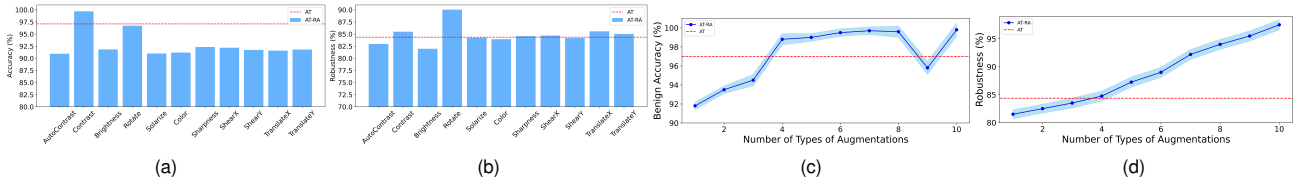


Figure 2: (a) Individual effects of single data augmentation method on benign accuracy. (b) Individual effects of single data augmentation method on adversarial robustness. (c) Influence of different combinations of data augmentation methods on benign accuracy. (d) Influence of different combinations of data augmentation methods on adversarial robustness.

randomly applies a series of augmentation operations from a set of 11 methods. However, the specific contribution of each data augmentation method to the model’s adversarial robustness is unclear. To address this, we conduct an ablation study to evaluate the individual impact of each augmentation method. Specifically, we limit the RA method set to a single type and enforce the use of the same data augmentation method for all training examples. The individual effects of each data augmentation method on benign accuracy are shown in Figure 2(a). It is clear that, except for the Contrast method, no single augmentation technique independently improves the benign accuracy.

Next, we analyze the results on adversarial robustness. The individual effects on adversarial robustness are shown in Figure 2(b). As seen in Figure 2(b), similar to the benign accuracy, no single augmentation method, except for the Rotate method, significantly improves adversarial robustness. The experimental results indicate that the diversity provided by individual data augmentation methods in adversarial training is insufficient to simultaneously improve both benign accuracy and adversarial robustness.

We also conduct the same experiments on fast adversarial training. The individual effects are presented in the Appendix, from which we can draw the same conclusion.

**Investigation on the Combined Effects of Data Augmentation Methods** Next, we investigate the impact of increasing the diversity of data augmentation types on adversarial robustness to explore the combined effects of data augmentation methods. In each experiment, we randomly select  $n$  augmentation types, where  $n \in \{n | 2 \leq n \leq 11, n \in \mathbb{Z}\}$ , to form the RA pool. The experimental results are shown in Figure 2(c). It can be observed that as more types of data augmentation methods are added to the RA pool, the benign accuracy continuously improves. Although oscillations occur at certain points, the overall trend remains unchanged. This trend suggests that a richer set of data augmentation categories increases the diversity of spectral domain information, allowing the model to learn more comprehensive representations, which in turn enhances benign accuracy.

Next, we analyze the impact on adversarial robustness. The experimental results are shown in Figure 2(d). It can be observed that as more types of data augmentation methods are added to the RA pool, adversarial robustness steadily improves. This trend suggests that a richer set of data augmentation categories not only increases the diversity of spectral domain information but also refines the spectral semantics of

hyperspectral images, enabling the model to learn more accurate representations, which in turn enhances its adversarial robustness.

The experimental results demonstrate that a richer set of data augmentation categories not only increases the diversity of spectral domain information but also refines the spectral semantics of hyperspectral images, enabling the model to learn more comprehensive and accurate features. As a result, this enhances both benign accuracy and adversarial robustness during adversarial training. Therefore, adopting the RandAugment method and utilizing a combination of data augmentation categories is both effective and necessary.

## 6 Conclusion

In this paper, we introduce adversarial training to the hyperspectral domain for the first time. Through extensive experiments, we demonstrate the effectiveness of adversarial training in a hyperspectral context. Our investigation uncovers the existence of the classification imbalance issue. As demonstrated by spectral analysis, this issue stems from adversarial noise and the non-smooth characteristics of adversarial examples. These factors distort or eliminate critical spectral semantic information, significantly impacting the deep learning model’s performance. To address this challenge, we incorporate RandAugment into adversarial training and propose a novel hyperspectral adversarial training method, AT-RA. Experimental results indicate that AT-RA not only enhances adversarial robustness but also improves benign accuracy. We further validate that this improvement applies to both traditional adversarial training and fast adversarial training methods. Finally, we conduct extensive ablation experiments on data augmentation strategies, demonstrating that the observed improvements stem from the increased spectral diversity and correction of spectral semantics in hyperspectral images. This validates the necessity of combining various data augmentation categories. Through our research, we contribute to advancing adversarial training in the hyperspectral domain, making it more adaptable and effective for engineering applications. This contribution provides a foundation for future research and practical implementations in hyperspectral analysis.

## References

[Akhtar *et al.*, 2021] Naveed Akhtar, Ajmal Mian, Navid Kardan, and Mubarak Shah. Advances in adversarial at-

tacks and defenses in computer vision: A survey. *IEEE Access*, 9:155161–155196, 2021.

[Bai *et al.*, 2021] Tao Bai, Jinqi Luo, Jun Zhao, Bihan Wen, and Qian Wang. Recent advances in adversarial training for adversarial robustness. *arXiv preprint arXiv:2102.01356*, 2021.

[Bai *et al.*, 2022] Tao Bai, Hao Wang, and Bihan Wen. Targeted universal adversarial examples for remote sensing. *Remote Sensing*, 14(22):5833, 2022.

[Bai *et al.*, 2024] Tao Bai, Yiming Cao, Yonghao Xu, and Bihan Wen. Stealthy adversarial examples for semantic segmentation in remote sensing. *IEEE Transactions on Geoscience and Remote Sensing*, 2024.

[Carlini and Wagner, 2017] Nicholas Carlini and David Wagner. Towards evaluating the robustness of neural networks. In *2017 ieee symposium on security and privacy (sp)*, pages 39–57. Ieee, 2017.

[Carmon *et al.*, 2019] Yair Carmon, Aditi Raghunathan, Ludwig Schmidt, John C Duchi, and Percy S Liang. Unlabeled data improves adversarial robustness. *Advances in neural information processing systems*, 32, 2019.

[Chen *et al.*, 2016] Yushi Chen, Hanlu Jiang, Chunyang Li, Xiuping Jia, and Pedram Ghamisi. Deep feature extraction and classification of hyperspectral images based on convolutional neural networks. *IEEE transactions on geoscience and remote sensing*, 54(10):6232–6251, 2016.

[Croce and Hein, 2020] Francesco Croce and Matthias Hein. Reliable evaluation of adversarial robustness with an ensemble of diverse parameter-free attacks. In *International conference on machine learning*, pages 2206–2216. PMLR, 2020.

[Cubuk *et al.*, 2020] Ekin D Cubuk, Barret Zoph, Jonathon Shlens, and Quoc V Le. Randaugment: Practical automated data augmentation with a reduced search space. In *Proceedings of the IEEE/CVF conference on computer vision and pattern recognition workshops*, pages 702–703, 2020.

[DeVries, 2017] Terrance DeVries. Improved regularization of convolutional neural networks with cutout. *arXiv preprint arXiv:1708.04552*, 2017.

[Goodfellow *et al.*, 2014] Ian J Goodfellow, Jonathon Shlens, and Christian Szegedy. Explaining and harnessing adversarial examples. *arXiv preprint arXiv:1412.6572*, 2014.

[Gowal *et al.*, 2021] Sven Gowal, Chongli Qin, Jonathan Uesato, Timothy Mann, and Pushmeet Kohli. Uncovering the Limits of Adversarial Training against Norm-Bounded Adversarial Examples, March 2021.

[Gu and Rigazio, 2015] Shixiang Gu and Luca Rigazio. Towards Deep Neural Network Architectures Robust to Adversarial Examples, April 2015.

[Han *et al.*, 2023] Chengxi Han, Chen Wu, Haonan Guo, Meiqi Hu, and Hongruixuan Chen. HANet: A hierarchical attention network for change detection with bitemporal very-high-resolution remote sensing images. *IEEE Journal of Selected Topics in Applied Earth Observations and Remote Sensing*, 16:3867–3878, 2023.

[He *et al.*, 2016] Kaiming He, Xiangyu Zhang, Shaoqing Ren, and Jian Sun. Deep residual learning for image recognition. In *Proceedings of the IEEE Conference on Computer Vision and Pattern Recognition*, pages 770–778, 2016.

[Hendrycks *et al.*, 2020] Dan Hendrycks, Norman Mu, Ekin D. Cubuk, Barret Zoph, Justin Gilmer, and Balaji Lakshminarayanan. AugMix: A Simple Data Processing Method to Improve Robustness and Uncertainty, February 2020.

[Jiang *et al.*, 2020] Pin Jiang, Aming Wu, Yahong Han, Yunfeng Shao, Meiyu Qi, and Bingshuai Li. Bidirectional adversarial training for semi-supervised domain adaptation. In *IJCAI*, pages 934–940, 2020.

[Lin *et al.*, 2024] Runqi Lin, Chaojian Yu, Bo Han, and Tongliang Liu. On the Over-Memorization During Natural, Robust and Catastrophic Overfitting, April 2024.

[Lu *et al.*, 2022] Xiaoyan Lu, Yanfei Zhong, and Liangpei Zhang. Open-source data-driven cross-domain road detection from very high resolution remote sensing imagery. *IEEE Transactions on Image Processing*, 31:6847–6862, 2022.

[Madry *et al.*, 2019] Aleksander Madry, Aleksandar Makelov, Ludwig Schmidt, Dimitris Tsipras, and Adrian Vladu. Towards Deep Learning Models Resistant to Adversarial Attacks, September 2019.

[Mou *et al.*, 2017] Lichao Mou, Pedram Ghamisi, and Xiao Xiang Zhu. Deep recurrent neural networks for hyperspectral image classification. *IEEE Transactions on Geoscience and Remote Sensing*, 55(7):3639–3655, 2017.

[Qi *et al.*, 2023] Jiahao Qi, Zhiqiang Gong, Xingyue Liu, Chen Chen, and Ping Zhong. Masked spatial–spectral autoencoders are excellent hyperspectral defenders. *IEEE Transactions on Neural Networks and Learning Systems*, pages 1–15, 2023.

[Qi *et al.*, 2024] Jiahao Qi, Zhiqiang Gong, Xingyue Liu, Chen Chen, and Ping Zhong. Masked spatial–spectral autoencoders are excellent hyperspectral defenders. *IEEE Transactions on Neural Networks and Learning Systems*, 2024.

[Rebuffi *et al.*, 2021] Sylvestre-Alvise Rebuffi, Sven Gowal, Dan Andrei Calian, Florian Stimberg, Olivia Wiles, and Timothy A. Mann. Data augmentation can improve robustness. *Advances in Neural Information Processing Systems*, 34:29935–29948, 2021.

[Ross and Doshi-Velez, 2018] Andrew Ross and Finale Doshi-Velez. Improving the adversarial robustness and interpretability of deep neural networks by regularizing their input gradients. In *Proceedings of the AAAI Conference on Artificial Intelligence*, volume 32, 2018.

[Roy *et al.*, 2023] Swalpa Kumar Roy, Ankur Deria, Dan-feng Hong, Behnood Rasti, Antonio Plaza, and Jocelyn

Chanussot. Multimodal fusion transformer for remote sensing image classification. *IEEE Transactions on Geoscience and Remote Sensing*, 61:1–20, 2023.

[Shi *et al.*, 2022] Cheng Shi, Yenan Dang, Li Fang, Zhiyong Lv, and Minghua Zhao. Hyperspectral image classification with adversarial attack. *IEEE Geoscience and Remote Sensing Letters*, 19:1–5, 2022.

[Shi *et al.*, 2023] Cheng Shi, Mengxin Zhang, Zhiyong Lv, and Qiguang Miao. Universal Object-Level Adversarial Attack in Hyperspectral Image Classification. *IEEE TRANSACTIONS ON GEOSCIENCE AND REMOTE SENSING*, 61, 2023.

[Shi, 2024] Cheng Shi. Attack-invariant attention feature for adversarial defense in hyperspectral image classification. *Pattern Recognition*, 2024.

[Tu *et al.*, 2023] Bing Tu, Wangquan He, Qianming Li, Yishu Peng, and Antonio Plaza. A new context-aware framework for defending against adversarial attacks in hyperspectral image classification. *IEEE Transactions on Geoscience and Remote Sensing*, 61:1–14, 2023.

[Wong *et al.*, 2020] Eric Wong, Leslie Rice, and J. Zico Kolter. Fast is better than free: Revisiting adversarial training, January 2020.

[Wu *et al.*, 2020] Dongxian Wu, Shu-Tao Xia, and Yisen Wang. Adversarial weight perturbation helps robust generalization. *Advances in neural information processing systems*, 33:2958–2969, 2020.

[Xiao *et al.*, 2022] Yi Xiao, Xin Su, Qiangqiang Yuan, Denghong Liu, Huanfeng Shen, and Liangpei Zhang. Satellite video super-resolution via multiscale deformable convolution alignment and temporal grouping projection. *IEEE Transactions on Geoscience and Remote Sensing*, 60:1–19, 2022.

[Xu and Ghamisi, 2022] Yonghao Xu and Pedram Ghamisi. Universal adversarial examples in remote sensing: Methodology and benchmark. *IEEE Transactions on Geoscience and Remote Sensing*, 60:1–15, 2022.

[Xu *et al.*, 2021a] Yonghao Xu, Bo Du, and Liangpei Zhang. Assessing the threat of adversarial examples on deep neural networks for remote sensing scene classification: Attacks and defenses. *IEEE Transactions on Geoscience and Remote Sensing*, 59(2):1604–1617, 2021.

[Xu *et al.*, 2021b] Yonghao Xu, Bo Du, and Liangpei Zhang. Self-attention context network: Addressing the threat of adversarial attacks for hyperspectral image classification. *IEEE Transactions on Image Processing*, 30:8671–8685, 2021.

[Xu *et al.*, 2023a] Yonghao Xu, Tao Bai, Weikang Yu, Shizhen Chang, Peter M. Atkinson, and Pedram Ghamisi. AI security for geoscience and remote sensing: Challenges and future trends. *IEEE Geoscience and Remote Sensing Magazine*, 11(2):60–85, 2023.

[Xu *et al.*, 2023b] Yonghao Xu, Tao Bai, Weikang Yu, Shizhen Chang, Peter M Atkinson, and Pedram Ghamisi. Ai security for geoscience and remote sensing: Challenges and future trends. *IEEE Geoscience and Remote Sensing Magazine*, 11(2):60–85, 2023.

[Xu *et al.*, 2024] Yichu Xu, Yonghao Xu, Hongzan Jiao, Zhi Gao, and Lefei Zhang. S<sup>3</sup>ANet: Spatial–Spectral Self-Attention Learning Network for Defending Against Adversarial Attacks in Hyperspectral Image Classification. *IEEE Transactions on Geoscience and Remote Sensing*, 62:1–13, 2024.

[Yang *et al.*, 2021] Shuo Yang, Zeyu Feng, Pei Du, Bo Du, and Chang Xu. Structure-aware stabilization of adversarial robustness with massive contrastive adversaries. In *2021 IEEE International Conference on Data Mining (ICDM)*, pages 807–816, 2021.

[Yang *et al.*, 2024] Cong Yang, Zuchao Li, and Lefei Zhang. Bootstrapping interactive image–text alignment for remote sensing image captioning. *IEEE Transactions on Geoscience and Remote Sensing*, 62:1–12, 2024.

[Yu *et al.*, 2024] Weikang Yu, Yonghao Xu, and Pedram Ghamisi. Universal adversarial defense in remote sensing based on pre-trained denoising diffusion models. *International Journal of Applied Earth Observation and Geoinformation*, 133:104131, 2024.

[Yun *et al.*, 2019] Sangdoo Yun, Dongyoon Han, Seong Joon Oh, Sanghyuk Chun, Junsuk Choe, and Youngjoon Yoo. Cutmix: Regularization strategy to train strong classifiers with localizable features. In *Proceedings of the IEEE/CVF International Conference on Computer Vision*, pages 6023–6032, 2019.

[Zhang and Zhang, 2022] Lefei Zhang and Liangpei Zhang. Artificial intelligence for remote sensing data analysis: A review of challenges and opportunities. *IEEE Geoscience and Remote Sensing Magazine*, 10(2):270–294, 2022.

[Zhang *et al.*, 2021] Lefei Zhang, Liangchen Song, Bo Du, and Yipeng Zhang. Nonlocal low-rank tensor completion for visual data. *IEEE Transactions on Cybernetics*, 51(2):673–685, 2021.

[Zhang *et al.*, 2022] Yaoyuan Zhang, Yu-an Tan, Tian Chen, Xinrui Liu, Quanxin Zhang, and Yuanzhang Li. Enhancing the transferability of adversarial examples with random patch. In *IJCAI*, pages 1672–1678, 2022.

[Zhang *et al.*, 2023] Jianping Zhang, Yung-Chieh Huang, Weibin Wu, and Michael R Lyu. Towards semantics-and domain-aware adversarial attacks. In *IJCAI*, pages 536–544, 2023.

[Zhang, 2017] Hongyi Zhang. Mixup: Beyond empirical risk minimization. *arXiv preprint arXiv:1710.09412*, 2017.

[Zhu *et al.*, 2024] Qiqi Zhu, Zhen Li, Tianjian Song, Ling Yao, Qingfeng Guan, and Liangpei Zhang. Unrestricted region and scale: Deep self-supervised building mapping framework across different cities from five continents. *ISPRS Journal of Photogrammetry and Remote Sensing*, 209:344–367, 2024.